Single-Turnover Kinetic Analysis of *Trypanosoma cruzi S*-Adenosylmethionine Decarboxylase†

Lisa N. Kinch and Margaret A. Phillips*

Department of Pharmacology, The University of Texas Southwestern Medical Center at Dallas, 5323 Harry Hines Boulevard, Dallas, Texas 75235-9041

Received June 29, 1999; Revised Manuscript Received December 31, 1999

ABSTRACT: *Trypanosoma cruzi S*-adenosylmethionine decarboxylase (AdoMetDC) catalyzes the pyruvoyl-dependent decarboxylation of *S*-adenosylmethionine (AdoMet), which is an important step in the biosynthesis of polyamines. The time course of the AdoMetDC reaction under single-turnover conditions was measured to determine the rate of the slowest catalytic step up to and including decarboxylation. Analysis of this single-turnover data yields an apparent second-order rate constant for this reaction of 3300 M^{-1} s^{-1} in the presence of putrescine, which corresponds to a catalytic rate of >6 s^{-1}. This rate is minimally 100-fold faster than the steady-state rate suggesting that product release, which includes Schiff base hydrolysis, limits the overall reaction. AdoMetDC exhibits an inverse solvent isotope effect on the single-turnover kinetics, and the pH profile predicts a pK_a of 8.9 for the basic limb. These results are consistent with a Cys residue functioning as a general acid in the rate-determining step of the single-turnover reaction. Mutation of Cys-82 to Ala reduces the rate of the single turnover reaction to 11 M^{-1} s^{-1} in the presence of putrescine. Further, a solvent isotope effect is not observed for the mutant enzyme. Reduction of the wild-type enzyme with cyanoborohydride traps the Schiff base between the enzyme and decarboxylated substrate, while little Schiff base species of either substrate or product was trapped with the C82A mutant. These data suggest that Cys-82 functions as a general acid/base to catalyze Schiff base formation and hydrolysis. The solvent isotope and pH effects are mirrored in single-turnover analysis of reactions without the putrescine activator, yielding an apparent second-order rate constant of 150 M^{-1} s^{-1}. The presence of putrescine increases the single-turnover rate by 20-fold, while it has relatively little effect on the affinity of the enzyme for product. Therefore, putrescine likely activates the *T. cruzi* AdoMetDC enzyme by accelerating the rate of Schiff base exchange.

S-Adenosylmethionine decarboxylase (AdoMetDC),[1] a key enzyme in the polyamine biosynthetic pathway, catalyzes the pyruvoyl-dependent decarboxylation of *S*-adenosylmethionine (AdoMet) (*1*). The product of this reaction donates aminopropyl groups to form the polyamines spermidine and spermine, which are essential for cell growth (*2*). In *Trypanosoma cruzi* AdoMetDC is the rate-limiting enzyme of this pathway (*3*, *4*), and a specific inhibitor of AdoMetDC reduces the ability of the parasites to infect host cells (*5*). Thus AdoMetDC is an attractive target for rational drug development.

AdoMetDC belongs to a group of enzymes that utilize a pyruvate cofactor for activity. Pyruvoyl-dependent enzymes generate this cofactor through an autoproteolytic cleavage into α and β subunits, leaving the pyruvate at the N-terminus of the α subunit (*6*). The mechanism of decarboxylation by pyruvate-dependent enzymes has been best characterized for histidine decarboxylase from *Lactobacillus* (*7*, *8*) and *Escherichia coli* AdoMetDC (*9*−*11*). The reaction (Scheme 1) begins with the substrate forming a Schiff base with the pyruvate cofactor (steps 1 and 2). The resulting imine promotes decarboxylation by serving as an electron sink for the carbanion produced upon removal of the carboxyl group (step 3). Following decarboxylation, the α-carbon is protonated (step 4), and the product is released by subsequent hydrolysis of the Schiff base (steps 5 and 6).

Previous biochemical analysis (*12*, *13*) as well as the recently reported crystal structure of the human AdoMetDC enzyme (*14*) has suggested the involvement of various residues in this catalytic mechanism. Mutation of several conserved residues including Glu-8, Glu-11, Cys-82, His-127, Glu-133, Ser-229, and His-243 significantly reduces AdoMetDC activity (*12*, *13*), with all but Glu-133 and His-127 found in proximity to the active site (*14*). Cys-82 has been implicated in protonation of the α-carbon prior to Schiff base hydrolysis (*13*), but the specific roles of each of the other residues in the reaction mechanism remain to be determined.

† This work was supported by grants from the National Institutes of Health (R01 AI34432), the Welch Foundation (I-1257), and the American Heart Association (M.A.P.) and the National Institutes of Health Biophysics Predoctoral Training Program (T32GM08297) (L.N.K.). M.A.P. is a recipient of a Burroughs Wellcome Fund Scholar Award in Molecular Parasitology.

* To whom correspondence should be addressed: Tel (214) 648-3637; Fax (214) 648-9961; e-mail philli01@utsw.swmed.edu.

[1] Abbreviations: AdoMetDC, *S*-adenosylmethionine decarboxylase; C82A AdoMetDC, mutant *Trypanosoma cruzi* enzyme in which the Cys residue that is structurally equivalent to Cys-82 in the human enzyme has been mutated to Ala; AdoMet, *S*-adenosylmethionine; $^{14}CO_2$-AdoMet, *S*-adenosyl-L-[*carboxyl*-^{14}C]methionine; $^{14}CH_3$-AdoMet, *S*-adenosyl-L-[*methyl*-^{14}C]methionine.

10.1021/bi991493r CCC: $19.00
Published on Web 03/02/2000

Scheme 1: Proposed Mechanism for Pyruvoyl-Dependent Decarboxylation of AdoMet

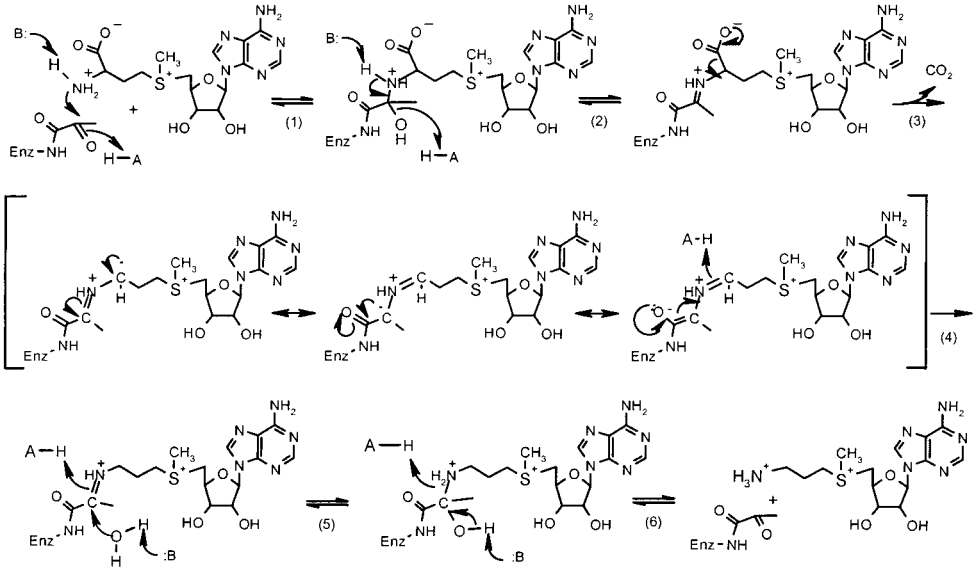

Although AdoMetDCs from different sources perform this same pyruvoyl-dependent reaction, their requirements for accomplishing the reaction differ considerably. The *E. coli* enzyme, which is thought to be structurally unrelated to the eukaryotic AdoMetDCs, requires a divalent metal ion for activity (*15*), while putrescine activates the yeast (*16*) and mammalian enzymes (*17, 18*). Other AdoMetDCs (*Tetrahymena*, some plants) do not exhibit activation with either divalent metal ions or putrescine (*19*). The *T. cruzi* enzyme is activated by cadaverine to the same extent as it is activated by putrescine. However the concentrations of either diamine required for maximal activity are considerably higher than those required for either the mammalian or the yeast enzyme (*20*). Additionally, the kinetics of activation appear to differ in these various systems. Addition of increasing amounts of a divalent cation to the *E. coli* enzyme increases V_{max} while it decreases K_m (*15*). Putrescine exerts its effects on the yeast enzyme by lowering K_m for substrate (*16*). In contrast, putrescine activates the *T. cruzi* enzyme by increasing V_{max} (*20*).

In this paper we further characterize the *T. cruzi* AdoMetDC kinetic mechanism and the effects of putrescine on this mechanism. We used single-turnover analysis to determine the rates of formation of intermediates through the decarboxylation step. The single-turnover rate is fast relative to the overall steady-state rate, suggesting that product release (in the form of Schiff base hydrolysis) is rate-limiting. Of the initial steps of the reaction, Schiff base formation appears to be slow relative to decarboxylation, and Cys-82 plays a crucial role as an acid catalyst in this step. Finally, the presence of putrescine increases the single-turnover rate approximately 20-fold while having relatively little effect on product affinity.

EXPERIMENTAL PROCEDURES

Materials. *S*-Adenosyl-L-[*carboxyl*-^{14}C]methionine ($^{14}CO_2$-AdoMet) and *S*-Adenosyl-L-[*methyl*-^{14}C]methionine ($^{14}CH_3$-AdoMet)were purchased from Amersham Pharmacia Biotech. All other reagents were purchased from Sigma unless otherwise stated.

Expression and Purification of T. cruzi AdoMetDC. AdoMetDC was expressed as a His-tagged fusion by use of the gene cloned from *T. cruzi* in a T7 bacterial expression construct (*20*). BL21/DE3 cells were grown in a New Brunswick BioFlo 3000 fermenter as previously described (*21*). Cell pellet (600 g) was frozen, and AdoMetDC was purified from 60 g aliquots by Ni^{2+}−agarose and Mono Q column chromatography (*20*). Stock protein solutions (0.4−0.8 mM) were stored in 50 mM HEPES, pH 8.0, 200 mM NaCl, and 2.5 mM DTT at −80 °C. Protein concentration was determined by absorbance at 280 nm with the previously determined extinction coefficient (*20*).

Generation and Characterization of C82A Mutant Enzyme. The structurally equivalent residue (based on amino acid sequence alignment) to human AdoMetDC residue Cys-82 in the *T. cruzi* enzyme is residue Cys-100. For consistency with prior literature, the human AdoMetDC numbering will be used to define the residue position number. A PCR-based site-directed mutagenesis was performed with the above expression plasmid as a template with the primers C82Af (5′-CGTATCATCCTGATCACAGCTGGCACGACGACTCAC-3′) and C82Ar (5′-GTGAGTCGTCGTG CCAGCTGTGATCAGGATGATACG-3′) as described (Stratagene QuikChange). The construct was verified by sequencing and the protein was expressed and purified as previously described (*20*).

Measurement of Single-Turnover Rates. Single-turnover rates were determined by mixing an excess of enzyme (0.04−0.6 mM) with $^{14}CO_2$-AdoMet (9 μM, 56 mCi/mmol), in the absence or in the presence of 10 mM putrescine, in 50 mM HEPES, pH 8.0, 200 mM NaCl, and 2 mM DTT. Reactions were initiated by adding enzyme to substrate in a final volume of 0.03 mL. The mixtures were then quenched with 6 M HCl (0.075 mL) after incubation at 37 °C for various times (0.5−42 s with putrescine or 2.5−1280 s without putrescine for wild-type AdoMetDC and 0−3 h for C82A). A metronome was used to time the addition of reagents allowing assay times as little as 0.5 s to be evaluated. Sodium bicarbonate was added to a final concentration of 5 mM, and reactions were incubated for an additional hour to release

all $^{14}CO_2$ from solution. As a control, zero time points were measured by adding 6 M HCl to the substrate prior to adding enzyme (at the shortest time point). The remaining $^{14}CO_2$-AdoMet concentration was quantitated by scintillation counting and data were analyzed as described below.

Measurement of Single-Turnover Rates in D_2O and at Various pHs. Reactions were performed essentially as described above. $^{14}CO_2$-AdoMet (56 mCi/mmol) was diluted 10-fold into either D_2O or H_2O and mixed with enzyme diluted into buffer (50 mM HEPES, pH 8.0, 100 mM NaCl, 5 mM DTT, and 0 or 10 mM putrescine) in D_2O or H_2O. The final concentrations of wild-type enzyme, C82A mutant enzyme, and substrate were 70, 150−250, and 9 μM, respectively, in approximately 80% D_2O (v/v). Single-turnover rates were determined at additional D_2O concentrations of 50% (v/v) and 66% (v/v) to extrapolate the isotope effect to 100% D_2O. Because identical enzyme concentrations were used, the ratio of the k_{obs} measured in H_2O and in D_2O corresponds to the ratio of k_2/K_S for each solvent. To determine the pH profile of the single turnover, reactions were carried out in 50 mM buffer (HEPES, pH 7.25−8.0, bicine, pH 8.25−9.0, CAPSO, pH 9.0−9.5), 100 mM NaCl, 3 mM DTT, and 10 mM putrescine. Some points included in the pH profile were carried out in 150 mM buffer. These points were duplicates of the data collected in 50 mM buffer and yielded the same rates, demonstrating that small changes in ionic strength do not affect the reaction rate.

Single-Turnover Kinetic Analysis. The release of $^{14}CO_2$ under single-turnover conditions (e.g., [E] ≫ [S]) follows first-order kinetics, and the data were fitted to eq 1a to obtain k_{obs} (the observed first-order rate constant for the decarboxylation of AdoMet):

$$S = S_0 \exp(-k_{obs}t) + S_\infty \quad (1a)$$

S is substrate concentration at time t, S_0 is initial substrate concentration, and S_∞ is substrate concentration at infinite time. The constant S_∞ was determined by averaging the amount of substrate remaining at six different time points, well after the initial burst phase was over. Under single-turnover conditions, observation of ES (or CO_2) from Scheme 2 (k_{obs}) is described by (*22*)

$$k_{obs} = \frac{k_2[E_0]}{K_S + [E_0]} \quad (1b)$$

The first-order rate constant k_2 is the rate of the slowest step of the reaction through decarboxylation and could be limited by the chemistry of Schiff base formation or by the actual decarboxylation step. K_S is defined as $(k_{-1} + k_2)/k_{+1}$ (Scheme 2). The plot of k_{obs} against enzyme concentration $[E_0]$ was linear and the apparent second-order rate constant k_2/K_S was determined from the slope of the line. Thus, only a lower limit for k_2 could be estimated.

Scheme 2

$$E + S \underset{k_{-1}}{\overset{k_{+1}}{\rightleftharpoons}} ES \xrightarrow{k_2} EP + CO_2 \xrightarrow{k_3} E + P$$

For the wild-type pL profile, the measured values of k_2/K_S at various pHs were fitted to eq 2a describing a system where two protons associate/disassociate cooperatively in both the acidic and basic limbs of the profile (*23*):

$$k_2/K_S = \frac{k_2/K_{S\ max}}{1 + 10^{(2\ pK_{a1} - 2\ pH)} + 10^{(2\ pH - 2\ pK_{a2})}} \quad (2a)$$

The parameter pK_{a1} represents the acidic limb, pK_{a2} represents the basic limb, and k_2/K_{Smax} represents the maximum predicted rate of the reaction. For the C82A mutant pL profile, the data were fitted to eq 2b describing a single proton association/disassociation for each limb:

$$k_2/K_S = \frac{k_2/K_{S\ max}}{1 + 10^{(pK_{a1} - pH)} + 10^{(pH - pK_{a2})}} \quad (2b)$$

Schiff Base Determination. To determine the extent of Schiff base formation on the enzyme, sodium cyanoborohydride ($NaCNBH_3$) was used as a reducing agent (*24*). The reaction mixtures contained AdoMetDC (0.2−0.4 mM) and either $^{14}CO_2$-AdoMet (56 mCi/mol, 44 or 90 μM) or $^{14}CH_3$-AdoMet (56 mCi/mmol, 44 or 90 μM) in 200 mM buffer (MES, pH 6.0; HEPES, pH 7.5; or bicine, pH 9.0) plus 10 mM putrescine, in a final volume of 0.02 mL. $NaCNBH_3$ was added to a final concentration of 200 mM, and the reactions were incubated for 20 min (wild-type enzyme) to 5 h (C82A mutant enzyme) at 37 °C. The protein was then precipitated by adding 7.5% TCA. The radioactivity was measured in both the precipitate and the supernatant to determine the extent of Schiff base formation. The precipitated protein was run on SDS−PAGE and stained with Coomassie blue. The extent of radioactive incorporation was visualized after addition EN^{3}HANCE autoradiography enhancer as recommended by the manufacturer (NEN Research Products) with a 6-day exposure.

Binding Analysis. Equilibrium product binding to AdoMetDC was measured by use of ultrafiltration to separate free ligand (*25*). Various concentrations of $^{14}CH_3$-AdoMet (10−120 μM, 56 mCi/mmol) were mixed with AdoMetDC (40 μM) in 50 mM HEPES, pH 8.0, 50 mM NaCl, and 2 mM DTT, with or without 10 mM putrescine (final volume 0.1 mL). Mixtures were left at room temperature for 2 h and then at 4 °C overnight so that all AdoMet was converted to product. A Microcon-10 microconcentrator (Amicon) was used to separate a small portion of free ligand (5−6 μL) from the total volume (100 μL) by spinning at 14000*g* for 7 s. The concentrations of free ligand $[L_f]$ and total ligand were determined by measuring radioactivity in an aliquot of sample (2 μL). Bound ligand concentration $[L_B]$ was calculated by subtracting free from total, and the data were fitted to eq 3 to determine the K_d (*23*):

$$[L_B] = \frac{[E][L_f]}{K_d + [L_f]} \quad (3)$$

Curve-Fitting Analysis. All data analysis to determine model-derived kinetic parameters was performed by nonlinear curve-fitting with Sigma Plot 4.0 (SPSS Inc., Chicago).

RESULTS

Single-Turnover Kinetic Analysis for T. cruzi AdoMetDC in the Presence and Absence of Putrescine. The measurement of AdoMetDC decarboxylation rates under conditions where enzyme is in excess of substrate allows the rate of the first

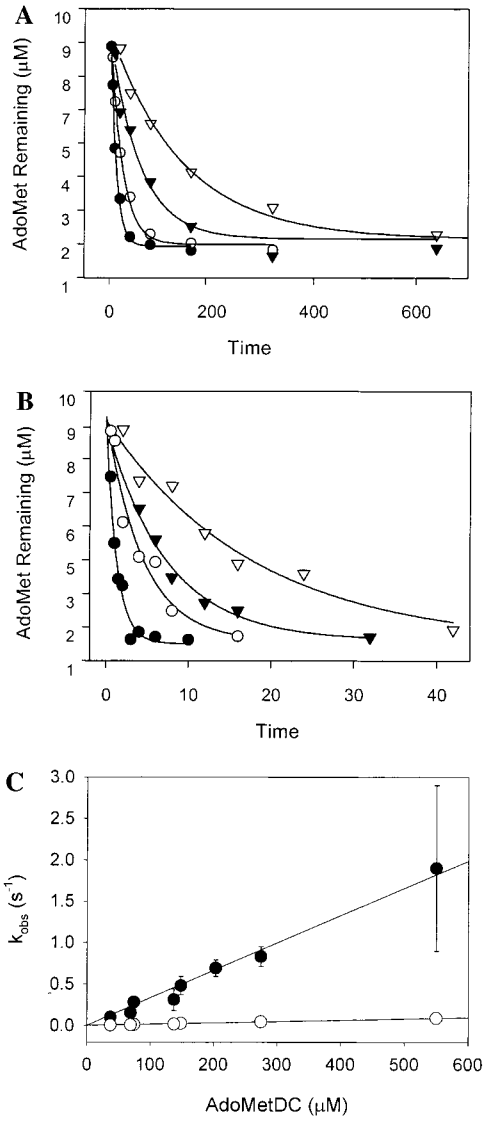

FIGURE 1: Single-turnover kinetic measurements in the absence of putrescine (panel A) or in the presence of 10 mM putrescine (panel B). Various concentrations of AdoMetDC 0.04 mM (▽), 0.075 mM (▼), 0.14 mM (○), and 0.28 mM (●) were mixed with 9 μM $^{14}CO_2$-AdoMet (56 mCi/mmol) at pH 8.0. Substrate remaining after quenching with 6 M HCl is plotted against time, and the data points are fitted to eq 1a describing a single-exponential decay (solid line). Panel C shows the dependence of k_{obs} on AdoMetDC concentration in the presence of 10 mM putrescine (●) or in the absence of putrescine (○). The data were fitted by linear regression, yielding apparent second-order rate constants (k_2/K_S) of 3300 M^{-1} s^{-1} in the presence of putrescine and 150 M^{-1} s^{-1} in the absence of putrescine. The error bars (panel C) represent the standard errors of the fits to eq 1a.

half of the reaction (k_2) to be kinetically isolated from that of product release (k_3) (Scheme 2). To determine the effect of the putrescine activator on the individual steps of the AdoMetDC reaction, we measured the time course of $^{14}CO_2$-AdoMet decarboxylation under single-turnover conditions in the absence and in the presence of saturating (10 mM) putrescine concentrations (Figure 1A,B). Each of these panels shows the decay of $^{14}CO_2$ from solution over time at four different enzyme concentrations. The decay follows first-order kinetics and plateaus at a nonzero value that is 25% of the original substrate concentration. The rates (k_{obs}) derived from fitting the decays to eq 1a were plotted against enzyme concentration (Figure 1C). The data have a linear dependence on enzyme concentration throughout the measured range (0.05−0.55 mM AdoMetDC), with slopes of 3300 M^{-1} s^{-1} and 150 M^{-1} s^{-1} in the presence and absence of putrescine, respectively. These values represent apparent second-order rate constants (k_2/K_S) for the reaction, with putrescine elevating the rate constant by 20-fold. The finding that the k_{obs} did not reach saturation over the range of enzyme concentrations tested prevents the determination of the individual rate constants (k_2 and K_S) from eq 1b. However, lower limits for these constants can be estimated. For a typical Michaelis−Menten curve, data are approximately linear up to 0.33 K_m (*26*), placing lower limits on the values of K_S and k_2 of 1.7 mM and 6 s^{-1} in the presence of 10 mM putrescine and 1.7 mM and 0.3 s^{-1} in the absence of putrescine, respectively.

Effect of D_2O and pH on Single-Turnover Kinetics. The single-turnover kinetic analysis presented above measures the slowest catalytic step of the AdoMetDC reaction up to and including decarboxylation (k_2). Upon consideration of the AdoMetDC catalytic mechanism (Scheme 1), k_2 can represent either Schiff base formation (steps 1 and 2) or decarboxylation (step 3). To gain further insight into the chemical nature of the step representing k_2 and to narrow the possible amino acid residues involved in this step, we measured the AdoMetDC single-turnover rates in D_2O and at various pL (Figure 2). Single-turnover decarboxylation occurs at a faster rate in D_2O (k_{obs} = 0.76 ± 0.09 s^{-1}) than in H_2O (k_{obs} = 0.37 ± 0.08 s^{-1}) under identical conditions in the presence of saturating putrescine concentrations (Figure 2A). The ratio of these rates corresponds to an inverse solvent isotope effect on k_2/K_S of 0.53 ± 0.16 (in 82% D_2O, pL 8.0). The inset of Figure 2A shows the effect of D_2O concentration on the k_2/K_S ratio, allowing for an extrapolation of the isotope effect to 100% D_2O ($^{H/D}k_2/K_S$ = 0.4 ± 0.12). Such an inverse solvent isotope effect on k_2/K_S arises from the reactant state of the free enzyme being destabilized relative to that of the transition state in a deuterium background, and it can be predicted by the fractionation factors (preference for hydrogen) of groups involved in kinetically significant proton transfers. A Cys residue on the free enzyme (fractionation factor = 0.55) functioning as a general acid in the transition state of the rate-determining step would explain the observed inverse isotope effect (*27*). In the absence of the putrescine activator, the same inverse rate trends (k_{obs} = 0.019 ± 0.003 s^{-1} in D_2O, k_{obs} = 0.01 ± 0.001 s^{-1} in H_2O) are observed (data not shown).

The AdoMetDC single-turnover decarboxylation rates depend strongly on pH. The single-turnover k_2/K_S rates (Figure 2B) increase as a function of pH with a slope of +2 to a maximum, and then they decrease with a slope of −2, suggesting a requirement for both a general base and a general acid in the reaction. The profile is consistent with a coupled two-proton transfer contributing to each ionization. Fits of the pH data to eq 2a yield an apparent maximum k_2/K_{Smax} of 4300 ± 700 M^{-1} s^{-1}, a pK_{a1} of 7.8 ± 0.1, and a pK_{a2} of 8.9 ± 0.1. Notably, the pK_{a2} of the basic limb predicted by eq 2 is consistent with the ionization of a Cys residue working as a general acid in the reaction. Due to the large dependence of AdoMetDC single-turnover decarboxylation on pH, the rates in D_2O were determined at various pD. The rates in D_2O were faster than the rates in H_2O at all pLs tested. Fitting of the pD profile to eq 2a yields a k_2/

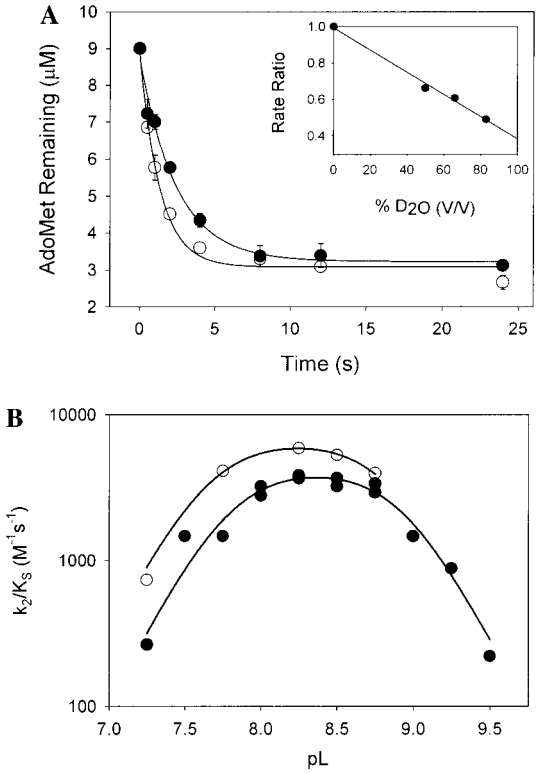

FIGURE 2: Wild-type AdoMetDC solvent isotope effects on the single-turnover kinetic reaction. Panel A shows the time courses for substrate decay at pL 8.0 in H_2O (●) and in 80% D_2O (○). Wild-type enzyme (0.07 mM) was mixed with $^{14}CO_2$-AdoMet (9 μM, 56 mCi/mmol) in the presence of saturating putrescine (10 mM). The data represent the average of two independent experiments with the standard deviation indicated by error bars and the line representing the fit to eq 1a. The rates in D_2O ($k_{obs} = 0.76 \pm 0.09$ s^{-1}) and in H_2O ($k_{obs} = 0.37$ $s^{-1} \pm 0.08$) were determined by averaging the fits for three independent time courses, with errors reported as the standard deviation. The inset shows the dependence of k_2/K_S on the percentage of D_2O used to extrapolate the isotope effect to 100% D_2O ($^Dk_2/K_S = 0.4$). Panel B shows the pL profile of k_2/K_S determined in H_2O (●) or in 80% D_2O (○). The solid and dotted lines represent the pH and the pD fits to eq 2a, respectively. The paramaters of the fits were determined to be $k_2/K_{Smax} = 4300 \pm 700$ M^{-1} s^{-1}, p$K_{a1} = 7.8 \pm 0.1$, and p$K_{a2} = 8.9 \pm 0.1$ in H_2O and $k_2/K_{Smax} = 6600 \pm 600$ M^{-1} s^{-1}, p$K_{a1} = 7.7 \pm 0.05$, and p$K_{a2} = 8.8 \pm 0.05$ in D_2O.

K_{Smax} of 6600 ± 600 M^{-1} s^{-1}, a pK_{a1} of 7.7 ± 0.05, and a pK_{a2} of 8.8 ± 0.05. Comparison of the apparent maximum rate in D_2O (6600 M^{-1} s^{-1}) with the rate in H_2O (4300 M^{-1} s^{-1}) produces an inverse isotope effect ($^{H/D}k_2/K_S = 0.6$, 80%D_2O) and verifies the data observed at a single pL ratio (Figure 2A). The pH profile in the absence of putrescine has similar inflection points (data not shown).

Analysis of Schiff Base Formation. The AdoMetDC reaction mechanism proceeds via Schiff base formation between substrate and enzyme prior to decarboxylation and is followed by hydrolysis of the Schiff base to release product (Scheme 1). To determine the extent of this Schiff base formation, we carried out $NaCNBH_3$ reduction in the presence of $^{14}CO_2$-AdoMet or $^{14}CH_3$-AdoMet. Upon reduction, the α subunit of AdoMetDC is covalently modified with radioactive AdoMet that has formed a Schiff base with the pyruvate cofactor (Figure 3). The two observed bands correspond to the α subunit of the AdoMetDC enzyme. The heterogeneity in mobility on SDS−PAGE of this subunit has also been seen for the mammalian enzyme (*28*). The presence

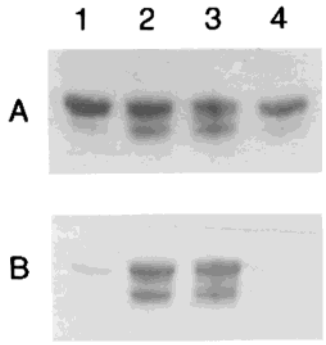

FIGURE 3: Sodium cyanoborohydride reduction of $^{14}CH_3$-AdoMet (lanes 1−3) and $^{14}CO_2$-AdoMet (lane 4) with AdoMetDC. Panel A shows a Coomassie blue stain of an SDS−15% polyacrylamide gel. The band represents the 32 kDa α subunit of AdoMetDC. Panel B shows a 6-day exposure of the same gel and represents the radioactive substrate covalently attached to the α subunit after reduction. Reduction mixtures contained wild-type AdoMetDC (0.17 mM) and substrate (56 mCi/mmol, 44 μM) at pH 6.0 (lane 1), pH 7.5 (lanes 2 and 4), and pH 9.0 (lane 3).

of the second band probably does not arise from proteolysis, and the samples have previously been shown to be 100% active (although they often run as a doublet) based on inhibitor titrations (*20*). Any radioactivity reductively fixed to the enzyme by $^{14}CH_3$-AdoMet is indicative of either product or substrate (lanes 1−3), while radioactivity reductively fixed to the enzyme by $^{14}CO_2$-AdoMet is indicative of substrate only (lane 4). By use of $^{14}CH_3$-AdoMet as a substrate in the reduction reaction, approximately 15% of the enzyme formed a Schiff base with $^{14}CH_3$-AdoMet at pH 6.0 (lane 1), while 70% formed a Schiff base at both pH 7.5 (lane 2) and pH 9.0 (lane 3) during the 20 min incubation. In contrast, no radioactivity was trapped after reduction of $^{14}CO_2$-AdoMet onto the enzyme at pH 7.5, suggesting that the substrate had been completely decarboxylated during the time of the experiment. These data suggest that an intermediate Schiff base complex of enzyme with decarboxylated substrate accumulates to a significant extent under the conditions of the experiment and are consistent with product release in the form of Schiff base hydrolysis being rate-limiting for the overall reaction.

Equilibrium Binding of Decarboxylated AdoMet. Due to the lack of saturation in the single-turnover analysis, the effects of the putrescine activator can only be extrapolated to the apparent second-order rate constant (k_2/K_S). To separate further the effects of putrescine on substrate (product) binding as opposed to its effects on catalysis, we incubated $^{14}CH_3$-AdoMet with wild-type AdoMetDC (0.042 mM) for sufficient time to convert 100% of substrate to product. The concentrations of bound and free ligand were determined by ultrafiltration, and the data were fitted to eq 3 to determine the dissociation constants for decarboxylated AdoMet in the presence ($K_d = 10 \pm 2$ μM) and absence ($K_d = 6 \pm 1$ μM) of putrescine (Figure 4). These data demonstrate that putrescine has little effect on the affinity of the enzyme for the product.

Single-Turnover Kinetic Analysis of the C82A Mutation in T. cruzi AdoMetDC. Results of the solvent isotope effect and pH studies on the single-turnover reaction suggest a critical role for a Cys residue in the first half of the AdoMetDC reaction. The crystal structure of human AdoMetDC shows Cys-82 to be in close proximity (within 4.4 Å) to

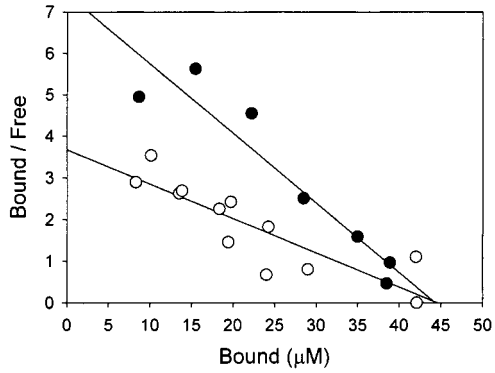

FIGURE 4: Schatchard plot of $^{14}CH_3$-AdoMet (10−120 μM) binding to AdoMetDC (42 μM). Free ligand was separated from total ligand using ultrafiltration, and concentrations were estimated by scintillation counting. Bound ligand was determined by subtracting the concentration of free ligand from the concentration of total ligand. Data in the presence of 10 mM putrescine (○) yielded a K_d of 10 ± 2 μM, and data in the absence of putrescine (●) yielded a K_d of 6 ± 1 μM, with error reported as the standard error of the linear fits.

the catalytic pyruvate moiety (*14*). Therefore, we mutated the structurally equivalent Cys residue to Ala in the *T. cruzi* enzyme to examine its role in the AdoMetDC reaction. The *T. cruzi* C82A mutant enzyme expresses to normal levels and is processed into α and β subunits, suggesting that the enzyme is correctly folded. The purified mutant enzyme decarboxylates AdoMet under single-turnover conditions with a 300-fold lower k_2/K_S (11 M^{-1} s^{-1}) at pH 8.0 than the wild-type enzyme in the presence of saturating putrescine (Figure 5A). In contrast to the wild-type enzyme, no solvent isotope effect is observed for the mutant enzyme over a range of pH and pD (Figure 5B). The inflection points of the acidic and basic limbs occur at similar pHs to the wild-type enzyme in both H_2O and D_2O. However, the slopes of both limbs are closer to −1, suggesting an uncoupling of the two proton transfers found in the wild-type profile. The data were fitted to eq 2b to determine k_2/K_{Smax} (37 ± 12 m^{-1} s^{-1}), pK_{a1} (8.2 ± 2), and pK_{a2} (8.4 ± 2) in H_2O (Figure 5B).

Under single-turnover conditions very little (<10%) Schiff base formation with decarboxylated substrate is detected on the mutant enzyme after either 20 min or 5 h of incubation (0.4 mM enyzme and 9 μM $^{14}CH_3$-AdoMet, pH 7.5) in the presence of $NaCNBH_3$. Additionally, virtually no Schiff base formation with substrate is detected (0.4 mM enyzme and 9 μM $^{14}CO_2$-AdoMet, pH 7.5) in the presence of $NaCNBH_3$. The substrate was completely decarboxylated during the incubation; thus, the enzyme is fully active in the reducing conditions. A similar incubation of histidine decarboxylase (with $NaCNBH_3$) also had no detrimental effect on enzyme activity (*29*). These data suggest that, unlike for the wild-type enzyme, the mutant enzyme does not significantly accumulate the Schiff base intermediate with decarboxylated substrate, nor does it accumulate any Schiff base species with substrate. This reduction data is consistent with slow Schiff base formation, followed by a more rapid decay of the intermediate, and suggests that the Cys mutation exerts its effects at this step.

DISCUSSION

Single-turnover kinetic analysis was used to study the reaction mechanism of *T. cruzi* AdoMetDC. The data suggest

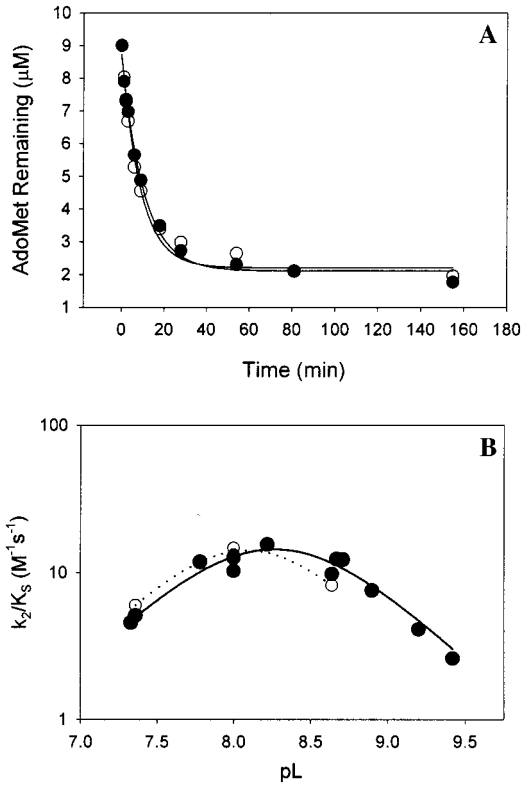

FIGURE 5: C82A mutant AdoMetDC solvent isotope effects on the single-turnover kinetic reaction. Panel A shows the time course of substrate decay at pL 8.0 in H_2O (●) and in 80% D_2O (○). C82A mutant enzyme (0.15 mM) was mixed with $^{14}CO_2$-AdoMet (9 μM, 56 mCi/mmol) in the presence of saturating putrescine (10 mM). The C82A rates in D_2O (k_{obs} = 0.12 ± 0.01 min^{-1}) and in H_2O (k_{obs} = 0.10 ± 0.01 min^{-1}) were determined from fits to eq 1a (solid line). Panel B shows the pL profile of k_2/K_S determined in H_2O (●) or in 80% D_2O (○). The solid and dotted lines show the pH and the pD fits to eq 2b, respectively. The parameters of the fits in H_2O are k_2/K_{Smax} = 37 ± 12 M^{-1} s^{-1}, pK_{a1} = 8.2 ± 2, and pK_{a2} = 8.4 ± 2.

that the reaction proceeds via two kinetically observable first-order steps (Scheme 2), where k_2 represents the slowest step of the reaction up to and including decarboxylation (Scheme 1, steps 1−3), and k_3 represents the slowest step after decarboxylation (Scheme 1, steps 4−6). For the mechanism defined in Scheme 2, the steady-state parameters (k_{cat} and K_m) are related to the individual rate constants k_2 and k_3 (*22*):

$$k_{cat} = \frac{k_2 k_3}{k_2 + k_3} \qquad K_m = K_S\left(\frac{k_3}{k_2 + k_3}\right) \tag{4}$$

Analysis of the single-turnover rates presented in this paper predicts a lower limit of 6 s^{-1} for k_2. This value is minimally 100-fold faster than the overall steady-state rate [k_{cat} of 0.06 s^{-1} (*20*)] at saturating concentrations of putrescine, demonstrating that neither Schiff base formation nor the decarboxylation step is rate-limiting for the overall reaction. The steady-state k_{cat} of 0.06 s^{-1} becomes a close approximation of k_3, suggesting that the rate-limiting step is either protonation of C_α or hydrolysis of the Schiff base to release product. Because $k_3 \ll k_2$, the majority of substrate present in the reaction will be in the form of EP. Thus, accumulation of a significant population of the ES species would require a high concentration of substrate. The finding that the K_S is minimally 1.7 mM, compared to a steady-state K_M of 0.09 mM (*20*), is predicted by eq 4.

Single-turnover analysis of the *T. cruzi* AdoMetDC reaction allows for the chemical steps through decarboxylation to be kinetically distinguished from those that follow decarboxylation. However, the resulting rate constant (k_2) may reflect either Schiff base formation or decarboxylation. The single-turnover pH profile data suggest that general acid catalysis is required in this step and that the required functional group has a pK_a (8.9) consistent with the ionization of a Cys residue. The observation of an inverse solvent isotope effect on the single-turnover reaction ($^{H/D}k_2/K_S = 0.4 \pm 0.12$) provides strong additional evidence that a Cys residue serves as a general acid in the transition state of this step. Cys is unique among the amino acids in displaying a fractionation factor ($\Phi = 0.55$) that is less than 1 (*27*). The involvement of thiol groups in acid/base catalysis has also been suggested by the observation of inverse solvent isotope effects for reactions catalyzed by homoserine transsuccinylase (*30*), and diaminopimelate epimerase (*31*). Because the chemistry involved in Schiff base formation requires general acid catalysis while the decarboxylation step does not, these data suggest that Schiff base formation is the rate-limiting step in the single-turnover reaction (k_2).

The interpretation of the solvent isotope effect data is further strengthened by the analysis of the data collected for the C82A mutant enzyme. A single Cys residue (Cys-82) is found in the active site of human AdoMetDC, for which the X-ray structure is available (*14*). Mutation of the structurally equivalent residue in the *T. cruzi* enzyme slows the single-turnover decarboxylation rate (k_2/K_s) 300-fold. Unlike for the wild-type enzyme, no solvent isotope effect is observed for the mutant enzyme. These data strongly implicate Cys-82 as the origin of the inverse solvent isotope effect in the wild-type enzyme. Furthermore, no detectable Schiff base species is formed between the mutant enzyme and either AdoMet or decarboxylated AdoMet. These data suggest that in the C82A mutant enzyme the rate of Schiff base formation is slower than the rate of its decay (decarboxylation). Taken together the data support the conclusion that Cys-82 is a general acid catalyst of Schiff base formation, which is the rate-limiting step in the first half of the reaction (k_2).

On the basis of a previous analysis of human C82A AdoMetDC, this Cys residue was proposed to serve as a general acid to protonate C_α after decarboxylation (*13*). However, the steady-state pH profiles (k_{cat}/K_M) reported for the human wild-type and C82A mutant enzymes are also consistent with a role of this residue in Schiff base formation. Because k_{cat}/K_M describes the reaction of free enzyme and free substrate up to the first irreversible step (decarboxylation), the steady-state k_{cat}/K_M pH profile provides information about the same part of the reaction as the single-turnover k_2/K_S pH profile. The basic limb pK_as for the human AdoMetDC steady state (p$K_a = 8.5 \pm 0.2$ (*13*)) and the *T. cruzi* AdoMetDC single turnover (p$K_a = 8.9$) are indeed similar, although the parasite enzyme shows a two-proton coupling. Further, the basic limb of the k_{cat}/K_m plot is no longer observed for the C82A mutant of human AdoMetDC, while the basic limb of the parasite C82A mutant enzyme reduces to a single proton transition. Thus, both the reported data on human AdoMetDC and our data on the *T. cruzi* enzyme support a role for Cys-82 as a general acid in Schiff base formation.

The role of Cys-82 is probably not limited to Schiff base formation. Mutation of human Cys-82 to Ala caused a significant decrease in k_{cat} (decreased by 2400-fold) and abolished the basic limb of the k_{cat} pH profile (*13*). Assuming this C82A mutation does not change the rate-determining step of human AdoMetDC, the disappearance of the k_{cat} basic limb would indicate that this residue is also important in the second half of the reaction (C_α protonation and Schiff base hydrolysis to release product). The common chemistry of the reaction steps involved in both k_2 and k_3 is Schiff base exchange, suggesting that the role of Cys-82 is to accelerate Schiff base formation in the first half of the reaction (k_2) and hydrolysis in the second half (k_3). Reduction of the wild-type enzyme with sodium cyanoborohydride traps a complex between enzyme and decarboxylated substrate, suggesting that an intermediate Schiff base species with product significantly accumulates. In contrast, very little Schiff base species of either substrate or product can be trapped on the C82A mutant *T. cruzi* enzyme during reduction, despite the fact that decarboxylation occurs. These data suggest that any catalytic step involving the decay of a Schiff base species (e.g., decarboxylation or C_α protonation) is unlikely to limit the rate of either the single-turnover or the steady-state reactions for the mutant enzyme (Scheme 1). Therefore, in addition to functioning as a general acid catalyst in Schiff base formation, Cys-82 probably assists in the second proton-transfer step of Schiff base hydrolysis (step 6).

The data on the activation of *T. cruzi* AdoMetDC by putrescine also support the hypothesis that common chemistry limits the rates in the two halves of the reaction mechanism. Putrescine greatly increases the apparent second-order rate constant (k_2/K_S) for *T. cruzi* AdoMetDC in the single turnover (20-fold), while having relatively little effect on the affinity of product for the enzyme. Analogously, putrescine increases k_{cat} (10-fold) while having little effect on K_m (*20*). Therefore putrescine presumably exerts its effects on catalytic steps and not on binding, increasing the single-turnover (k_2) and steady-state (k_3) rates to a similar extent. If putrescine accelerates Schiff base hydrolysis by 10-fold, this step must be minimally 10-fold faster than protonation. In the case of ornithine decarboxylase, protonation of the α-carbon to form product is associated with a rate constant that is at least 2 orders of magnitude faster than any other step after decarboxylation (*21*). Histidine decarboxylase of *Lactobacillus* provides another example of a reaction where the rate of protonation is thought to be fast relative to formation of free product (*32*). Like the *E. coli* AdoMetDC, this pyruvate-dependent decarboxylase retains stereochemical configuration about the α-carbon upon protonation (*9*, *32*), suggesting a similar protonation mechanism for these two enzymes. Analogously, this step may be fast for *T. cruzi* AdoMetDC, such that k_3 describes the hydrolysis of the Schiff base complex.

The single-turnover analysis presented in this paper provides a detailed kinetic understanding of the reaction mechanism of *T. cruzi* AdoMetDC. The overall steady-state rate of the reaction is limited by product release in the form of Schiff base hydrolysis, while the first half of the reaction is limited by Schiff base formation. This basic knowledge is essential to the interpretation of any isotope or pH studies performed on the enzyme, as illustrated by the conclusion that the residue Cys-82 plays a kinetically significant catalytic

role in Schiff base exchange. Additionally, these results lead to a hypothesis on the mechanism of putrescine activation. Since we know that putrescine affects the catalytic steps of Schiff base exchange, and not equilibrium binding of product, putrescine may lower the pK_a of the Cys residue involved in Schiff base exchange by stabilizing the Cys anion. Further elucidation of this hypothesis concerning putrescine activation of the *T. cruzi* AdoMetDC enzyme is currently under investigation.

ACKNOWLEDGMENT

We thank H. Brooks and A. Osterman for helpful discussions and E. Ross for critical reading of the manuscript.

REFERENCES

1. Stanley, B., and Shantz, L. (1994) *Biochem. Soc. Trans. 22*, 863−869.
2. Heby, O., and Persson, L. (1990) *Trends Biochem. Sci. 15*, 153−158.
3. Ariyanayagam, M., and Fairlamb, A. (1997) *Mol. Biochem. Parasitol. 84*, 111−121.
4. Le Quesne, S., and Fairlamb, A. (1996) *Biochem. J. 316*, 481−486.
5. Yakubu, M., Majumder, S., and Kierszenbaum, F. (1993) *J. Parasitol. 79*, 525−532.
6. van Poelje, P. D., and Snell, E. E. (1990) *Annu. Rev. Biochem. 59*, 29−59.
7. Recsei, P. A., and Snell, E. E. (1970) *Biochemistry 9*, 1492−7.
8. Gallagher, T., Snell, E. E., and Hackert, M. L. (1989) *J. Biol. Chem. 264*, 12737−43.
9. Allen, R. R., and Klinman, J. P. (1981) *J. Biol. Chem. 256*, 3233−9.
10. Markham, G., Tabor, C., and Tabor, H. (1983) in *Methods in Enzymology* (Tabor, H., and Tabor, C. W., Eds.) Vol. 94, pp 228−230, Academic Press, New York.
11. Wickner, R. B., Tabor, C. W., and Tabor, H. (1970) *J. Biol. Chem. 245*, 2132−9.
12. Pegg, A. E., Xiong, H., Feith, D. J., and Shantz, L. M. (1998) *Biochem. Soc. Trans. 26*, 580−6.
13. Xiong, H., Stanley, B. A., and Pegg, A. E. (1999) *Biochemistry 38*, 2462−70.
14. Ekstrom, J. L., Mathews, II, Stanley, B. A., Pegg, A. E., and Ealick, S. E. (1999) *Structure 7*, 583−595.
15. Markham, G. D., Tabor, C. W., and Tabor, H. (1982) *J. Biol. Chem. 257*, 12063−8.
16. Poso, H., Sinervirta, R., and Janne, J. (1975) *Biochem. J. 151*, 67−73.
17. Zappia, V., Carteni-Farina, M., and Della Pietra, G. (1972) *Biochem. J. 129*, 703−709.
18. Sakai, T., Hori, C., Kano, K., and Oka, T. (1979) *Biochemistry 18*, 5541−5548.
19. Poso, H., Hannonen, P., Himberg, J., and Janne, J. (1976) *Biochem. Biophys. Res. Commun. 68*, 227−234.
20. Kinch, L. N., Scott, J. R., Ullman, B., and Phillips, M. A. (1999) *Mol. Biochem. Parasitol. 101*, 1−11.
21. Brooks, H. B., and Phillips, M. A. (1997) *Biochemistry 36*, 15147−55.
22. Hiromi, K. (1979) *Kinetics of fast enzyme reactions*, Halsted Press, New York.
23. Segel, I. H. (1975) *Enzyme Kinetics*, John Wiley & Sons, Inc., New York.
24. Borch, R. F., Bernstein, M. D., and Durst, H. D. (1971) *J. Am. Chem. Soc. 93*, 2896−2904.
25. Sophianopoulos, J. A., Durham, S. J., Sophianopoulos, A. J., Ragsdale, H. L., and Cropper, W. P., Jr. (1978) *Arch. Biochem. Biophys. 187*, 132−7.
26. Copeland, R. A. (1996) *Enzymes, A Practical Introduction to Structure, Mechanism, and Data Analysis*, VCH Publishers, Inc., New York.
27. Quinn, D., and Sutton, L. (1991) in *Enzyme mechanism from isotope effects* (Cook, P. F., Ed.) pp 73−126, CRC Press, Inc., Boca Raton, FL.
28. Stanley, B., Shantz, L., and Pegg, A. (1994) *J. Biol. Chem. 269*, 7901−7907.
29. Recsei, P. A., and Snell, E. E. (1982) *J. Biol. Chem. 257*, 7196−202.
30. Born, T. L., and Blanchard, J. S. (1999) *Biochemistry 38*, 14416−23.
31. Koo, C. W., and Blanchard, J. S. (1999) *Biochemistry 38*, 4416−22.
32. Rose, I. A., and Kuo, D. J. (1992) *Biochemistry 31*, 5887−92.

BI991493R